EPJ AP
Applied Physics
www.epj.org

Eur. Phys. J. Appl. Phys. **41**, 221–227 (2008) DOI: 10.1051/epjap:2008025

Electrical properties and transport mechanisms of p-znte/n-si heterojunctions

M.A.M. Seyam, H.T. El-Shair and G.F. Salem

EDP SCIENCES

The title "The European Physical Journal" is a joint property of EDP Sciences, Società Italiana di Fisica (SIF) and Springer

Eur. Phys. J. Appl. Phys. **41**, 221–227 (2008)
DOI: 10.1051/epjap:2008025

THE EUROPEAN PHYSICAL JOURNAL
APPLIED PHYSICS

Electrical properties and transport mechanisms of p-znte/n-si heterojunctions

M.A.M. Seyam[a], H.T. El-Shair, and G.F. Salem

Department of Physics, Faculty of Education, Ain Shams University, Roxy, 9004 Cairo, Egypt

Received: 21 August 2007/ Accepted: 3 January 2008
Published online: 9 April 2008 –

Abstract. Zinc telluride thin films have been deposited on glass and silicon wafers substrates at room temperature by thermal evaporation technique in a vacuum of 10^{-5} Torr. The thickness dependence of both the dc electrical resistivity and thermoelectric power of ZnTe were carried out at room temperature and after being annealed over a thickness range from 22 nm to 170 nm. The type of conduction, the carriers concentration and the conduction mechanisms were revealed. The average thermal activation energy ΔE equals to 0.324 eV for the as deposited films and 0.306 eV for annealed films, it is found to correspond with the ionization energy reported for intrinsic defect levels in ZnTe. Seebeck coefficient measurements showed that ZnTe thin films behave as p-type semiconductor and the average value of the free charge carrier concentration is found to be 1.6×10^{19} cm^{-3}. The built-in voltage, the width of the depletion region, the diode quality factor and the operating conduction mechanisms have been determined from dark current-voltage ($I-V$) and capacitance-voltage ($C-V$) characteristics of p-ZnTe/ n-Si heterojunctions.

PACS. 73.40.Lq Other semiconductor-to-semiconductor contacts, p-n junctions, and heterojunctions – 74.25.Fy Transport properties – 72.20.-i Conductivity phenomena in semiconductors and insulators

1 Introduction

Zinc telluride is a promising semiconductors material of II-VI group for fabrication of high efficiency solar cells and other optoelectronic devices due to its suitable intrinsic energy gap, 2.26 eV [1–4]. Photoluminescence study on ZnTe and optoelectronic detection of THz radiation carried out in recent years [5,6]. Zinc telluride thin films have been prepared by thermal evaporation at room temperature were found to behave as p-type semiconductors and with a positive thermopower coefficient and they were crystallized in a polycrystalline nature [7–10].

Hall measurements yielded hole mobility values in the range between 0.1 and 1 cm^2/V s for both as deposited and annealed films [11].The activation energy of ZnTe films is deduced from the temperature dependence of dark conductivity, it was found to be 0.5 eV and the hole concentration equals 10^{17} cm^{-3} [11,12]. The conductivity of ZnTe thin films at room temperature was found to change from 0.45 to 0.14 Ω^{-1} cm^{-1} with the variation of deposition temperature in the rang 300 K to 633 K and a hole carrier concentrations of ZnTe films were found to be 1.6×10^{19} cm^{-3} [8,9,13]. The photoluminescence measurements of the heterojunctions of ZnSe were found through hole injection from the p-type ZnTe into the n-type ZnSe and the three deep hole trap level have been observed in the depletion region of p-ZnTe/ n-CdTe heterojunction [14]. The as-deposited ZnTe films of high resistive with activation energy of 0.48 eV in the temperature range 240 K to 300 K were investigated by [15]. The defects in ZnSe /ZnTe multiple quantum well-based pseudo-ohmic contacts to p-ZnSe were studied by [16] and the role of the buffer layer in the active junction in amorphous-crystalline silicon heterojunction solar cells was studied by [17]. In this paper, an attempt has been made to see the correspondence of the dark $I-V$ and $C-V$ characteristics of p-ZnTe/ n-Si heterojunctions and the thermal activation processes in ZnTe thin films.

2 Experimental techniques

ZnTe thin films were deposited on an optically flat precleaned glass and silicon wafers substrates with the help of a high vacuum-coating unit (Edwards type E 306 A) at the vacuum 10^{-5} Torr. Pure (99.999%) bulk ZnTe obtained from BALZERS was used to deposit the thin films with deposition rate equals to 6 nms^{-1}. The substrate temperatures were fixed at 300 K. Thin tantalum boat was used as source heater. The film thickness were measured by Tolansky's method [18]. Also the rate of deposition and the films thickness were controlled using a quartz crystal thickness monitor (Model FTM4, Edwards co, England). Electrical resistivity measurements of ZnTe thin films of

[a] e-mail: Seyam80@yahoo.com

different thicknesses before and after being annealed in vacuum of 10^{-5} Torr were performed in the temperature range of 300 K to 450 K using the tow probe technique. The ohmic contacts were made by evaporating high purity indium electrodes through a suitable mask onto the films. The ohmic nature of the contacts was confirmed by the linear $I-V$ characteristics throughout the above mentioned temperature range. Thin film resistance of samples was measured directly using an electrometer (Keithly 617). Thermoelectric power was measured using the differential technique, as reported in [19].

p-ZnTe/n-Si heterojunction can be prepared according to the following steps:

i- The silicon wafers of n-types of conductivity were etched using CP_4 etching solution for 1.5 min. (CP_4 etching solution is prepared by adding 18 ml of HF acid to 1.5 ml of acetic acid and 57 ml conc. HNO_3).
ii- After etching, the silicon wafers are washed for two minutes by distilled water and then by ethyl alcohol.
iii- The silicon wafers after being etched and cleaned are coated from one side by a gold electrode while the other side was coated by p-ZnTe thin film of different thicknesses. ZnTe coating is over coated by a gold mesh to be used as the other electrode.
iv- The prepared p-ZnTe/n-Si heterojunction was annealed for one hours at 473 K to complete the junction formation.

Dark $I-V$ and $C-V$ characteristics of p-ZnTe/n-Si heterojunction were measured at room temperature using model 410 $C-V$ Meter.

3 Results and discussions

3.1 Electrical resistivity

Temperature dependence of dark electrical resistivity of ZnTe thin films with different thicknesses ranges from 22 nm to 170 nm in the temperature range from 300 K to 450 K for as deposited samples and after annealing samples at 473 K for one hour in vacuum are shown in Figure 1a, b. The thermally activated electrical resistivity is

$$\rho = \rho_\circ e^{\frac{\Delta E}{kT}} \quad (1)$$

$\rho_\circ$ where is the pre-exponential factor(Ω cm), ΔE is the thermal activation energy of the conduction electrons (eV), k is the Boltzmann's constant and T is the temperature in Kelvin. The graphs (Fig. 1a) exhibited one linear part indicating one impurity level of energy ΔE, the values of which recorded in Table 1. It was found that the activation energy decreases with increasing the film thickness due to the increase of the grain size from 53.4 to 83 nm this proved by X-ray analysis [20].

It is also clear that the obtained values of ΔE are close to the ionization energy reported for intrinsic defect levels in ZnTe (0.25 eV) [11,21], suggesting that the acceptor levels dominating electrical conduction are most likely the levels originating from Zn vacancies which was detected by

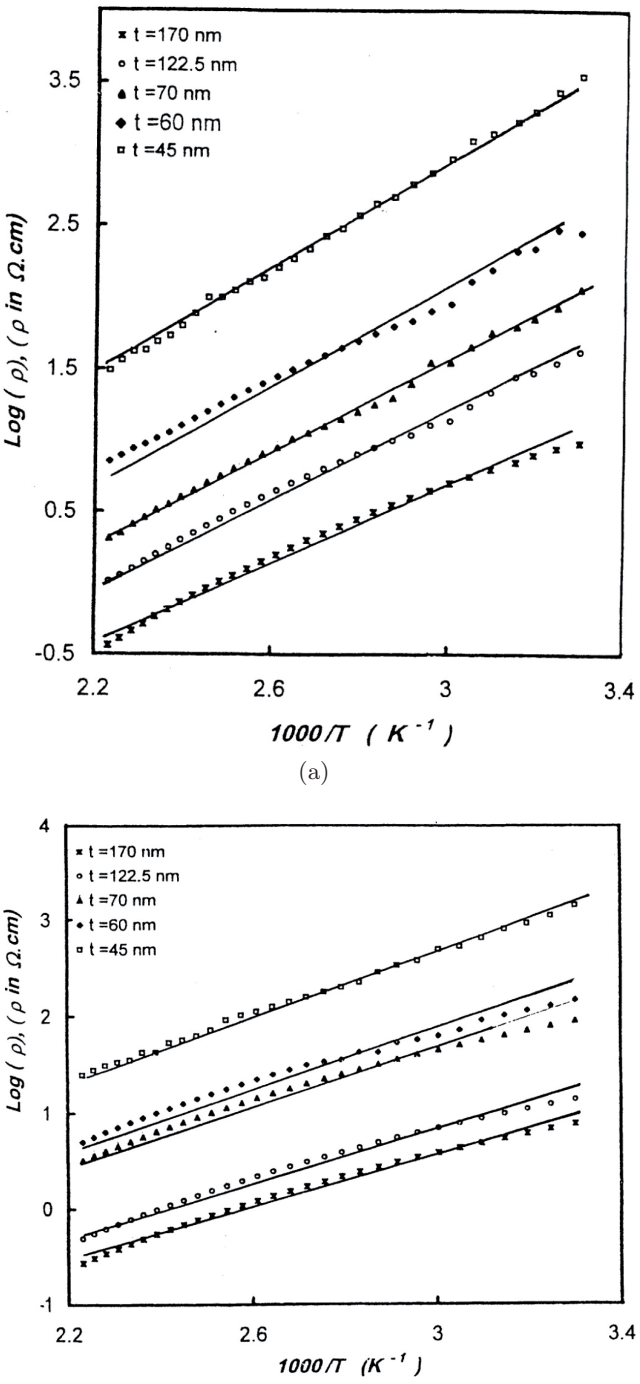

Fig. 1. The dark electrical resistivity versus the reciprocal temperature for ZnTe of different thickness (a) as-deposited samples and (b) annealed samples.

EDX analysis [20]. ZnTe films were found to be p-types owing to acceptor levels associated with Zn vacancies present in the film.

The dark electrical resistivity as a function of temperature for the above mentioned samples after being annealed for one hour at 473 K have the same behavior with small decreasing on the electrical resistivity and the activation

Table 1. ΔE of p-ZnTe films for different thicknesses expressed in eV for the as-deposited and after annealing.

Thicknesses of samples (nm)	45	60	70	122.5	170	
ΔE (as-deposited samples)	0.360	0.350	0.320	0.312	0.278	From resistivity
	0.320	0.300	0.280	0.270	0.250	From thermopower
ΔE (after annealing samples) at 473 K	0.343	0.32	0.31	0.288	0.269	From resistivity
	0.300	0.300	0.270	0.260	0.269	From thermopower

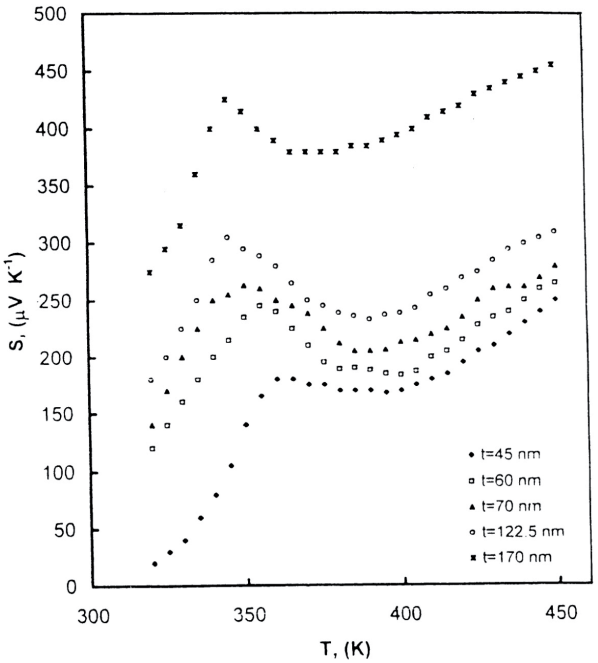

(a)

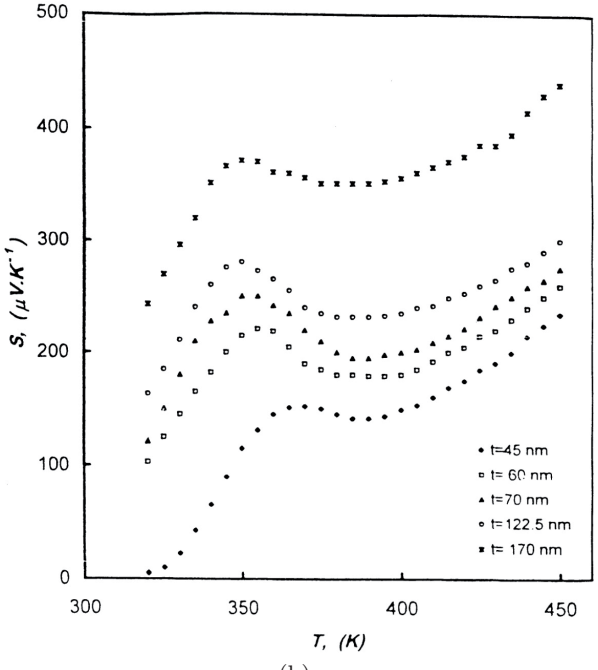

(b)

Fig. 2. Thermoelectric power, S, versus the temperature, T, for ZnTe of different thickness (a) as-deposited samples and (b) annealed samples.

energy in comparison with the as deposited samples can be detected as shown in Figure 1b and Table 1. The activation energy of the as-deposited samples is bit higher than that of the annealed samples might be due to the grain growth in addition to the release of defects. Accordingly the quality of the film improves with annealing. Consequently the carriers move more easily and hence the activation energy tends to decrease.

4 Thermoelectric power

Temperature dependence of thermoelectric power, S, created in ZnTe thin films, of different thicknesses from 45 nm to 170 nm within the temperature range of 300 K to 450 K for as deposited samples and after annealing samples at 473 K for one hour in vacuum are shown in Figure 2a, 2b. Seebeck coefficient S for as deposited samples depends strongly on the film thickness as shown in Figure 2a. The variations of S with temperature for all samples have the same behavior and a positivity nature. This indicates that ZnTe thin films behave as p-type semiconductor. The Seebeck coefficient S as a function of temperature for the above mentioned samples after being annealed have the same behavior with small decreasing on the Seebeck coefficient can be observed as shown in Figure 2b. The Seebeck coefficient tends to increase with increase film thickness as shown from Figure 2a, 2b. The values of Seebeck coefficient S were used to calculate the free charge carrier concentration p at different temperatures according to the relation:

$$P = 2(2\pi m^* kT/h^2)^{3/2} \exp(2 - Se/k) \qquad (2)$$

where $m^* = 0.26m_o$ [8], T is the absolute temperature expressed in Kelvin, h is the Planck constant (6.63×10^{-34} J s), e is the charge of electron (1.6×10^{-19} C), k is the Boltzmann's constant (1.38×10^{-23}J/K) and S is the Seebeck coefficient in Volt/K. From the analysis of temperature dependence of the free charge carrier concentration p for ZnTe thin films before and after annealing respectively. We found that the values of ΔE are computable with the values obtained from the resistivity measurements and the value of the free charge carrier concentration varies from 3.14×10^{19} cm^{-3} to 1.11×10^{18} cm^{-3}, with film thickness 45 nm and 170 nm respectively. ΔE of p-ZnTe films for different thicknesses expressed in eV for the as-deposited and after annealing which deduced from electrical measurements and those from thermopower were record in Table 1. The discrepancy between the values deduced from electrical measurements and those from thermopower; such discrepancy seems to be obvious and has

Table 2. values of ξ and I_S for p-ZnTe /n-Si heterojunction at different temperatures.

T(K)	ξ	$I_S(10^{-6}\text{A})$
300	1.93	3.700
323	1.77	4.200
343	1.67	5.400
363	1.58	7.200
383	1.50	13.95

been in many articles [22] and can be attributed to nature of carriers. In the electrical resistivity the current carriers are due to electric field while in thermopower the current carriers are due to temperature gradient thermal current.

5 Current voltage characteristics of P-ZnTe/n-Si Heterojunction

The dark $I-V$ characteristics for p-ZnTe/n-Si heterojunction in the temperature range 300–403 K with p-ZnTe thickness of 170 nm as representative example is shown in Figure 3a. The forward current at low forward bias shows an exponential increases with the applied voltage, but at high forward bias is a liner behavior. This behavior indicates a clear effect of the junction series resistance. It is clear that the junction exhibits rectifying characteristics showing a p-n diode-like behavior for all the measuring temperature. The rectification ratio at ± 1 V was approximately 4 at room temperature. The experimental results of junction resistance R_J against voltage V are shown in Figure 3b for p-ZnTe/n-Si heterojunction. As shown in Figure 3b at sufficiently high forward bias, the junction resistance approaches a constant value is equal to the series resistance R_s. On the other hand, the junction resistance is also constant, at sufficiently reverse bias, which is equal to the diode shunt resistance R_{sh}. The obtained values of R_S and R_{Sh} are found to be 300 Ω and 1420 Ω respectively. Figure 4 shows the dark forward current versus applied voltage over the temperature range 300 K to 405 K. The variation of log I and V can be represented by the classical relation [23]:

$$I = I_s[\exp(\text{eV}/\xi kT) - 1] \tag{3}$$

where ξ is the diode quality factor, k is the Boltzmann, s constant and I_S is the saturation current. From these characteristics, the junction parameters of the saturation current I_s and the diode quality factor ξ were evaluated. It was observed that the saturation current increases with temperature showing that thermo ionic emission may be responsible for the dominant charge transport mechanism across the junction. The obtained values of ξ and I_S at different temperatures are listed in Table 2.

It is clear that the junction was non ideal in showing $\xi > 1$, which may be attributed to the recombination of electrons and holes in the depletion region, and also to the increased effect of the different current on increasing applied voltage [23].

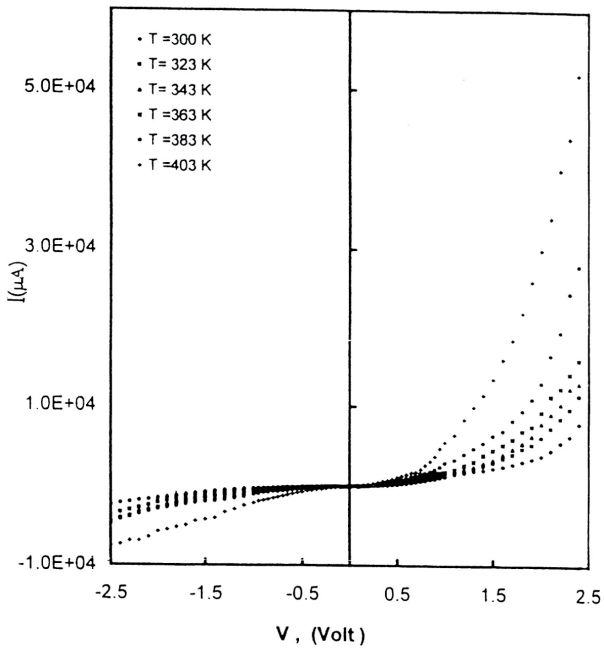

(a)

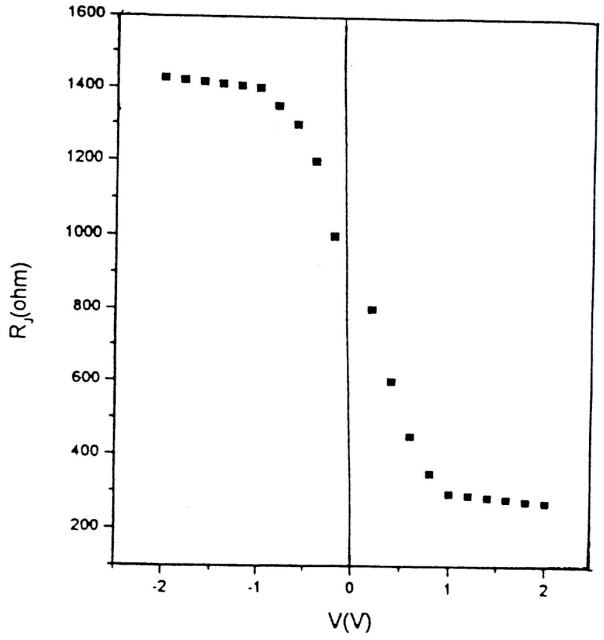

(b)

Fig. 3. (a) $I-V$ characteristics for p-ZnTe/n-Si heterojunction in both forward and reverse bias. (b) Junction resistance, R_J against V for p-ZnTe/n-Si heterojunction.

To confirm that the thermionic emission is the operating conduction mechanism in the low biasing voltage region, more analysis must be carried out. According to the thermionic conduction, the saturation current is given by [23]:

$$I_s = AA^*T^2 \exp(-\phi_b/kT) \tag{4}$$

where A is the diode effective area and, A^* is the Richardson's constant, ϕ_b is the potential barrier height.

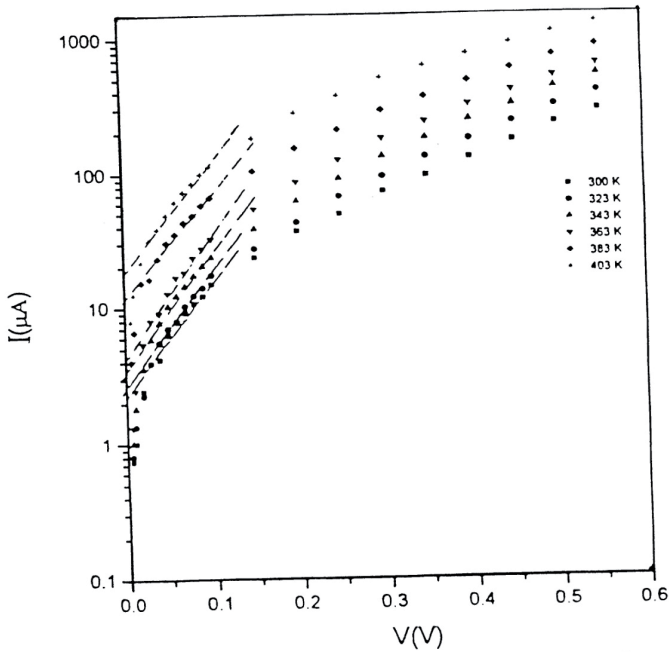

Fig. 4. Semi-logarithmic plots of the forward bias $I-V$ curves for p-ZnTe/n-Si heterojunction cell at different temperature.

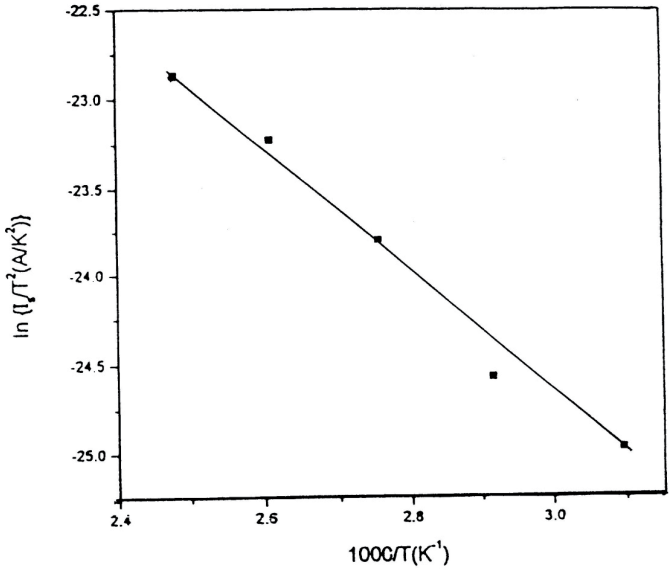

Fig. 5. The variation of I_s/T^2 against $1000/T$ for p-ZnTe/n-Si heterojunction.

The temperature dependence of the saturation current is shown in Figure 5. The linearity of the $\ln(I_s/T^2)$ versus the $1/T$ plot indicates that the operating mechanisms is the thermo ionic emission. From the slope of the plot the value of potential barrier height ϕ_b was found to be 0.28 eV.

Under relatively high foreword voltage, other mechanism becomes dominant between $0.2 < V < 0.7$ V, the current shows a power dependence on voltage, i.e. follows the relation $I\alpha\ V^m$ [24], as shown in Figure 6, where $m \sim 2$. Such power dependence suggests that I is a space-

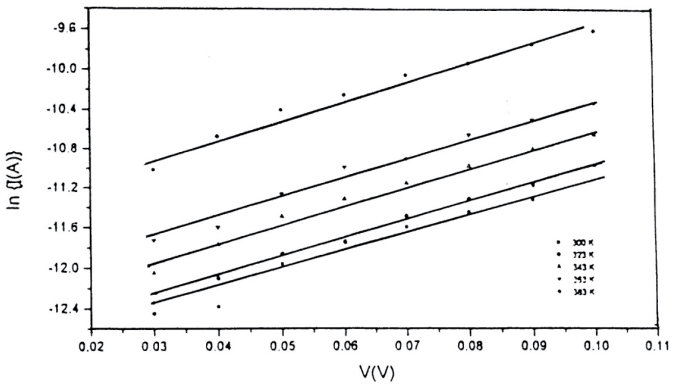

Fig. 6. Ln I against Ln V at higher voltage bias for p-ZnTe/n-Si heterojunction.

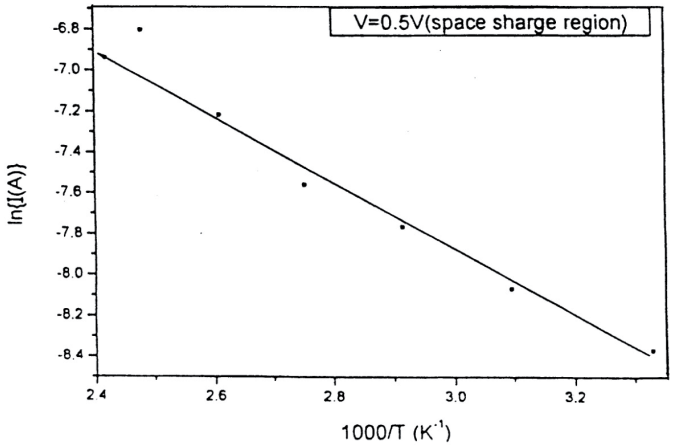

Fig. 7. Ln I versus $1000/T$ for p-ZnTe/n-Si heterojunction, at 0.5 V.

charge-limited current (SCLC) and permits that utilization of SCLC theory in the $I-V$ analysis. Thus, it is possible to recognize that the effect of traps on the conduction current which is dominated by discrete trapping level [25]. The current, I in this region is given by the familiar expression [23].

$$I_{SCL} = 9A\varepsilon\varepsilon_o\mu V^2 N_v \exp(-E_t/kT)/8t^3 N_t \qquad (5)$$

where ε is the permittivity of p-ZnTe film, ε_0 is the permittivity of free space, μ is the hole mobility, t is the thickness of ZnTe film, N_v is the effective density of states in the valance band and N_t is the total trap concentration situated at an energy level E_t above the valence band edge.

However, the slope of the plot of ln I versus $1000/T$ as shown in Figure 7 is used to evaluate E_t which has a value of 0.15 eV.

6 Capacitance voltage characteristics of p-ZnTe/n-Si Heterojunction

Figure 8 shows the dark $C^{-2}-V$ characteristics of the P-ZnTe/n-Si heterojunction device measured at room temperature in the reverse direction. As shown in this figure,

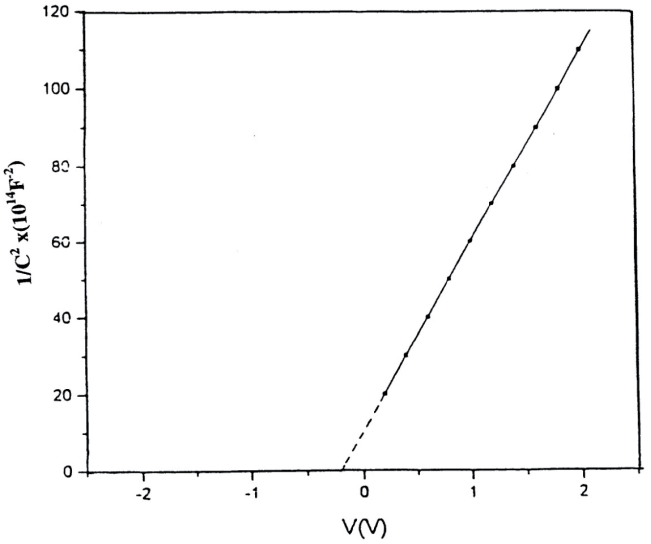

Fig. 8. Plots of $1/C^2$ versus V for P-ZnTe/n-Si heterojunction, measured at one MHz.

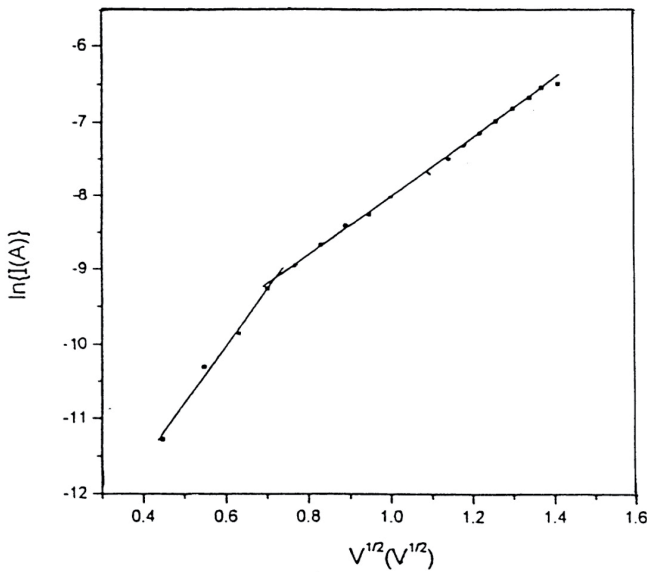

Fig. 9. Ln I against $V^{1/2}$ in reverse bias.

it is clear that C^{-2} increases linearly with voltage. Consequently, the carrier concentration is homogeneous and the linearity of the $C^{-2} - V$ plot indicates that the junction is abrupt [26], and the free carrier concentration, N, could be calculated from the slope shown in Figure 8 and using the relation [23]:

$$d(C^{-2})/dV = -2/\varepsilon\varepsilon_o e N a^{*2} \qquad (6)$$

where a^* is the effective area of the device (0.5 cm^2). The derived value of N was found to be 1.2×10^{17} cm^{-3} and the intercept of the line C^{-2} versus V on the abscissa essentially gives the diffusion voltage, V_d, which equals 0.23 V. The capacitance of the device C_o at zero bias was found to be ∼33 nF, which corresponds to a thickness d_s of the depletion region ($d_s = \varepsilon\varepsilon_o a^*/C_o$) of 90 nm.

The reverse bias $I - V$ characteristics as a function of temperature plotted in the form of ln I against $V^{1/2}$ are shown in Figure 9. It can be seen from the figure that these are two distinct regions for each characteristics, which may be interpreted in terms of either Schottky effect or the Pool- Frenkel effect. $I - V$ expressions for these processes given by [27,28]:

$$I = AA^*T^2 \exp(\phi_s/kT) \exp(\beta_s V^{1/2}/kTd_s^{1/2}) \qquad (7)$$

for the Pool-Frenkel effect, where ϕ_s is the Schottky barrier height, I_0 is the lower-field current and β_s and β_{pf}, the Schottky and Pool-Frenkel field-lowering coefficients, respectively. Theoretical values of these coefficients are given by [26]:

$$I = I_o \exp(\beta_{pf} V^{1/2}/kTd_s^{1/2}),\ \ 2\beta_s = \beta_{pf} = (e/\pi\varepsilon\varepsilon_o)^{1/2}. \qquad (8)$$

This gives $\beta_s = 1.46 \times 10^{-5}$ eV m$^{1/2}$ V$^{-1/2}$ and $\beta_{pf} = 2.92 \times 10^{-5}$ eV m$^{1/2}$ V$^{-1/2}$. Using the d_s value of 90 nm, obtained from the capacitance measurement, the mean values of β from the slopes of Figure 9 may be obtained and were found to be 5.59×10^{-5} eV m$^{1/2}$ V$^{-1/2}$ and 2.92×10^{-5} eV m$^{1/2}$ V$^{-1/2}$ for lower and higher voltage range respectively. The former value is at variance with that expected for Schottky or Pool-Frenkel effect, being 2.04 times the theoretical value of β_{pf} and double this factor for β_s. This was accounted for the non-uniform fields within the structure [29]. Similar behaviour has been reported previously for n-Cd S $_{0.5}$Se$_{0.5}$/ p-In P [30] and n-ZnSe /p-Si [31] heterojunction cells and also for other Schottky junction photovoltaic devices [23–26]. The value of the barrier height Φ_s from Figure 9 was found to be 0.32 eV, which coincides within experimental error, with the value of 0.28 eV obtained from the slope of Figure 7.

7 Conclusions

The dark electrical resistivity of ZnTe films indicating the existence of one activation energy $\Delta E = 0.324$ and 0.306 eV before and after annealing respectively. Seebeck coefficient measurements showed that ZnTe thin films behave as p-type semiconductors. The value of the free charge carrier concentration varies from 3.14×10^{19} cm^{-3} to 1.11×10^{18} cm^{-3}, with film thickness 45 nm and 170 nm respectively.

The series R_S,the shunt resistance R_{sh}, the diode quality factor ξ, the saturation current (I_S), the diffusion voltage, V_d, and the operating conduction mechanism were estimated from the analysis of the $C - V$ characteristics and the $I - V$ characteristics of the p-ZnTe/n-Si heterojunction.

The authors acknowledge the help of Prof. A.A. El Shazly and Dr. A.M. Ibrahim, Physics department, Faculty of education, Ain shams university for their support and help throughout this work.

References

1. R. Sarma, N. Mazumdar, H.L. Das, Bull. Mater. Sci. **29**, 15 (2006)
2. T. IShizaki et al., J. Phys. D Appl. Phys. **37**, 255 (2004)
3. D.W. Kim, J.S. Kwak, H.S. Park, H.N. Kim, S.M. Lee, C.S. Kim, S.K. Noh, H.K. Baik, J. Electron. Mater. **26**, 83 (1997)
4. J.T. Trexler, J.J. Fijol, L.C. Calhoun, R.M. Park, P.H. Holloway, J. Electron. Mater. **25**, 9 (1996)
5. P.C. Kalita, K.C. Sarma, H.L. Das, J. Assam Sci. Soc. **39**, 117 (1998)
6. M. Nishio, T. Enoki, Y. Mitsuighi, Q. Guo, H. Ogawa, Thin Solid Films, **343**, 288 (1999)
7. P.K. Kalita, B.K. Sarma, H.L. Das, Indian J. Pure Appl. Phys. **37**, 399 (1999)
8. B. Maiti, P. Gupta, S. Chaudhuri, A.K. Pal, Thin Solid Films. **239**, 104 (1994)
9. D. Noda, T. Aoki, Y. Nakanishi, Y. Hatanaka, Vacuum **15**, 619 (1998)
10. M. Nishio, G. Qixin, H. Ogawa, Thin Solid Films **343**, 508 (1999)
11. R.G. Bohn, C.N. Tabory, C. Deak, M. shoa, A.D. Compaan, *IEEE First World Conf. Photovoltaic Energy Conversion, 1994*, 354
12. L. Feng, D. Mao. J. Tang, R.T. Collins, J.U. Trefny, J. Electron. Mater. **25**, 1422 (1996)
13. S. Bhunia, D.N. Bose, Delhi, India: Narosa Publishing House. **1**, 158 (1998)
14. M.R.H. Khan, M. Saji, J. Appl. Phys. **57**, 4668 (1985)
15. H. Bellakhder, A. Outzourhit, E.L. Ameriane, Thin Solids Film **382**, 30 (2001)
16. S. Tomiya, S. Kijima, H. Okuyama, H. Tsukamoto, T. Hino, S. Taniguchi, H. Noguchi, E. Kato, A. Ishibashi, J. Appl. Phys. **86**, 3616 (1999)
17. J. Pallares, R.E.I. Schropp, J. Appl. Phys. **88**, 293 (2000)
18. S. Tolansky, *Multiple-bem, Interferometry of Surface and Films* (London, Oxford, 1988), 147
19. A.A. El Shazly, D. Abd Elhady, H.S. Metwally, M.A.M. Seyam, J. Phys. Cond. Matter **10**, 5943 (1998)
20. H.T. El-Shair, M.A.M. Seyam, G.F.A. Salem, Eur. Phys. J. Appl. Phys., in press
21. K. Mochizuki, A. Jerano, M. Momose, A. Taike, M. Kawata J. Gotoh, S. Nakatsuka, J. Appl. Phys. **78**, 3216 (1995)
22. S.A. Mazen, A. Elfalaky, H.A. Hashem, Appl. Phys. A **61**, 559 (1995)
23. A.S. Riad, M. EL-Shabasy, R.M. Abdel-Latif, Thin Solid Films **235**, 222 (1993)
24. A.S. Riad, Physica B **270**, 148 (1999)
25. T.L. Chu, S.S. Chu, F. Firszt, J. Appl. Phys. **29**, 4 (1986)
26. A.K. Hassan, R.D. Gould, Int. J. Electron **69**, 11 (1990)
27. R.D. Gould, B.B. Ismail, Vacuum **50**, 99 (1998)
28. N.G. Patel, J. Mater. Science **21**, 2097 (1986)
29. T.G. Abdel-Malik, A.A. Ahmed, A.S. Riad, Phys. Stat. Sol. (a) **121**, 507 (1990)
30. S. Darwish, H.S. Soliman, A.S. Riad, Thin Solid Films **259**, 248 (1995)
31. S. Darwish, A.S. Riad, H.S. Soliman, Semicond. Sci. Technol. **11**, 96 (1996)